TRACKING FAST-ROLLING LEUKOCYTES *IN VIVO* WITH ACTIVE CONTOURS

Nilanjan Ray and Scott T. Acton

Virginia Image and Video Analysis (VIVA)
Department of Electrical and Computer Engineering,
University of Virginia, Charlottesville, VA 22904
{nray, acton}@virginia.edu

ABSTRACT

In this paper we propose and demonstrate an active contour technique to track fast-rolling leukocytes observed *in vivo* from video microscopy. A rolling leukocyte is an activated white blood cell that interacts with the vessel wall (the endothelium) in the inflammatory process. Tracking is enhanced here to accommodate fast-moving cells. To tackle the task of tracking wherein only low temporal resolution is possible, we have introduced an energy-minimizing framework and obtained a partial differential equation (PDE) based active contour evolution technique. The proposed PDE's are shown to be an initialization-insensitive version of the gradient vector flow (GVF) proposed by Xu and Prince. We modify the GVF-PDE's by adding a Dirichlet type boundary condition (BC) based on the initial position of the active contour and the direction of cell movement. Using actual intravital experiments, we compare the performance of the proposed active contour tracker with the Dirichlet BC, the active contour tracker *without* the BC, the correlation tracker and the centroid tracker. The comparative results provide evidence of the advantages of the proposed method in terms of increased number of frames successfully tracked and reduced localization error.

1 INTRODUCTION

Tracking leukocytes *in vivo* provides vital information to research groups that are studying inflammatory disease [1,2]. In discovering, developing and validating potential novel anti-inflammatory treatments the analysis of leukocyte rolling is emerging as an important tool. As an example, E-selectin inhibitors can decrease the number and increase the velocity of rolling leukocytes in living animals [3]. Faster rolling leukocytes indicate weaker, fewer, or shorter-lived bonds between the rolling cell and the endothelial lining of the inflamed vessel. Currently, the analysis of rolling velocities is laborious and requires tens of hours of user-interactive image processing work after each experiment. In a single hour of experimentation, more than 100,000 frames of video data are produced. To manually inspect each frame for leukocyte position recording is clearly impossible. We seek automated methods of leukocyte tracking to obtain leukocyte positions and to compute leukocyte velocities.

To meet such requirements, we have proposed a shape-size constrained active contour based tracker. The associated energy has a constraint term that penalizes the deviation of the snake from a prescribed circular shape and size [4]. Our snake tracker, however, is limited in the sense that the cell cannot move more than one cell radius per video frame. In this work we enhance tracking fast rolling cells through an enhancement of the basic GVF flow [5,6] that permits tracking of faster-rolling leukocytes. The improvements allow us to double the maximum speed of cells tracked from approximately 100 μm/s to 200 μm/s. Specifically, we have designed an energy functional based on the initial snake position and the direction of movement of the cell. This energy functional is convex and thus the minimization leads to the globally optimal solution.

In the next section, we introduce the active contour approach. Section 3 explains background for GVF, and Section 4 illustrates the motivation behind the enhanced GVF. In section 5 we compare the proposed enhanced GVF-snake tracking performance with the non-enhanced GVF-snake tracker and with two standard trackers – the centroid [7] and correlation [8] trackers.

2 ACTIVE CONTOUR APPROACH

Let us define a 2D curve via the normalized arc-length parameter $s \in [0,1]$ as $C(s)=[x(s),y(s)]$. A parametric active contour/snake is such a 2D curve, closed or open, that can move over the image plane as a result of two competing forces – internal force, which tries to maintain the smoothness of the contour and the external force that is computed from the image data. The external force can be so defined that the active contour gets locked onto certain image features (e.g., edges) while moving over the image plane. This process is realized in practice through the minimization of the following energy functional [9]:

$$E_s = \int_0^1 \left(\frac{1}{2}\left\{\alpha|\mathbf{C}'(s)|^2 + \beta|\mathbf{C}''(s)|^2\right\} + E_{\text{ext}}(\mathbf{C}(s))\right) ds, \qquad (1)$$

where the first and the second term in the integral represent, respectively, the internal and the external energy. Minimization of (1) leads to the Euler equations [9]:

$$\alpha\mathbf{C}''(s) - \beta\mathbf{C}''''(s) - \nabla E_{\text{ext}}(\mathbf{C}(s)) = \mathbf{0}. \qquad (2)$$

Furthermore (2) can be thought of as a force balance equation where the internal force, $\alpha\mathbf{C}''(s) - \beta\mathbf{C}''''(s)$, acts against the external force, $-\nabla E_{ext}(\mathbf{C}(s))$, to nullify each other [5]. The snake moves in accordance with these forces. With this view (2) can be written as

$$\alpha\mathbf{C}''(s) - \beta\mathbf{C}''''(s) + (u,v) = \mathbf{0}, \qquad (3)$$

where (u,v) is the external force used for moving the snake.

3 AN EXTERNAL FORCE – GVF

An external snake force proposed by Xu and Prince is the gradient vector flow (GVF) field (u,v) and is defined through the minimization of the following energy functional [5,6]

$$E_{GVF}(u,v) = \frac{1}{2}\iint g(|\nabla f|)(u_x^2 + u_y^2 + v_x^2 + v_y^2)dxdy + \frac{1}{2}\iint (1-g(|\nabla f|))((u-f_x)^2 + (v-f_y)^2)dxdy, \quad (4)$$

where f is the edge map, and g is monotonically decreasing [6]:

$$f(x,y) = |\nabla G_\sigma(x,y) * I(x,y)|, \quad (5)$$

$$g(|\nabla f|) = \exp(-(\frac{|\nabla f|}{K})). \quad (6)$$

K, a positive constant, controls the smoothness of the resulting field [6]. One obtains the following Euler equations by minimizing (4) by way of the variational principle [6]:

$$\begin{aligned} g\nabla^2 u - (1-g)(u-f_x) &= 0, \\ g\nabla^2 v - (1-g)(v-f_y) &= 0. \end{aligned} \quad (7)$$

GVF has some attractive properties such as its ability to attract the snake toward edges from a relatively long distance [5,6].

4 ENHANCED GRADIENT VECTOR FLOW

4.1 Motivation

To illustrate the sensitivity of GVF snakes to the initial position, we provide Figure 1a, which depicts the snake evolution (black contours) starting from an initial snake (white contour) inside the gray circle. The driving (u, v) force for this snake is GVF and is given in Figure 2. The reason behind the failure of the snake to recover the circle is that the initial snake does not include the medial axis (in this case the center) [10].

A similar experiment on an *in vivo* video frame further emphasizes the need for enhancing GVF. Figure 3a shows a video frame obtained *in vivo* and a snake (white contour) capturing a leukocyte. Figure 3b shows the fast-rolling leukocyte in the next video frame, where the initial snake (white) is the final snake obtained in the previous frame. The snake used here utilizes a shape-size constraint that is biased toward roughly circular shapes of an approximate radius [4]. Figure 3b shows that, instead of capturing the cell, the snake (black contour) drifts away. The reason for the failure is the low temporal resolution or equivalently the high frame-to-frame cell displacement for which the initial snake does not include the cell center. The GVF force field, in this case, guides the snake away from the cell.

4.2 Enhancing GVF through Dirichlet BC

We now propose an external force (u,v), constraining the GVF-PDE's [6] through Dirichlet BC's as follows. Let D be the rectangular image domain with boundary ∂D and C be the region bounded by the initial closed snake with boundary ∂C. Then our proposed enhanced GVF-PDE's become:

$$\left.\begin{aligned} g\nabla^2 u - (1-g)(u-f_x) &= 0 \\ g\nabla^2 v - (1-g)(v-f_y) &= 0 \end{aligned}\right\} \text{ when } (x,y) \in (D-C)$$
$$(u,v) = \mathbf{n}, \text{ when } (x,y) \in \partial C \text{ and}$$
$$\nabla(u,v) = \mathbf{0}, \text{ when } (x,y) \in \partial D. \quad (8)$$

Here $\mathbf{n}$ is a vector that specifies the constraining Dirichlet BC. If we want to capture the circle with the initial snake shown in Figure 1a, we can specify $\mathbf{n}$ as the unit normal to the boundary ∂C, since the object is stationary (see result in Figure 1b). The underlying enhanced GVF field is shown in Figure 4. For capturing the leukocyte with the initial snake shown in Figure 3b we use $\mathbf{n}$=(-1,0), *i.e.*, biasing the flow in the direction of motion. In Figure 5, the snake is seen to have recovered the position of the fast-rolling leukocyte.

Although the proposed enhanced GVF has some similarity to the pressure-force/balloon snake [11], the former is quite sensitive to the image edge strength. Figure 6a depicts how the pressure-snake "leaks" through a weaker edge. Figure 6b shows the proposed modified GVF snake that recovers the strong as well as the weak intensity edges. The GVF-PDE smoothly interpolates the solution between the BC and the gradient of the edge-map. Thus the GVF-PDE enables the snake to "sense" the edge strength, whereas the pressure snake has no such mechanism to foresee the gradient magnitude in its path.

4.3 Convex Energy Functional

For applying the proposed enhanced GVF snake to tracking fast-rolling cells, we may use the following Dirichlet BC in (8): $\mathbf{n} = (v_0^x, v_0^y)$, which is the estimated direction of movement for the tracked leukocyte (equal to the direction of flow in the observed venule). We can view this as a *drift bias* as the following analysis shows. Since, $\mathbf{n}$ is now constant with respect to the space variables (x, y), (8) can be achieved through an energy minimization framework explaining the intuition behind our proposed enhancement. Let (p, q) define a new flow that is related to the original flow, (u, v) and the drift bias (v_0^x, v_0^y), as follows:

$$u = p + v_0^x, \; v = q + v_0^y. \quad (9)$$

Substituting (9) in (8) we get:

$$\left.\begin{aligned} g\nabla^2 p - (1-g)(p + v_0^x - f_x) &= 0 \\ g\nabla^2 q - (1-g)(q + v_0^y - f_y) &= 0 \end{aligned}\right\} (x,y) \in (D-C)$$
$$(p,q) = \mathbf{0}, \text{ when } (x,y) \in \partial C \text{ and}$$
$$\nabla(p,q) = \mathbf{0}, \text{ when } (x,y) \in \partial D. \quad (10)$$

This new formulation can be viewed as the addition of a soft constraint biased in the direction of leukocyte motion. Thus we can define the enhanced GVF energy functional as follows:

$$E_{\text{GVF-enhanced}}(p(x,y),q(x,y),v^x,v^y) = \frac{1}{2}\iint g(|\nabla f|)\left(p_x^2+p_y^2+q_x^2+q_y^2\right)dxdy + \frac{1}{2}\iint (1-g(|\nabla f|))((p+v^x-f_x)^2+(q+v^y-f_y)^2)dxdy + \frac{1}{2}\lambda((v^x-v_0^x)^2+(v^y-v_0^y)^2). \quad (11)$$

Here, λ is a constant expressing the degree to which the drift bias (v^x,v^y) is close to the actual estimated cell movement direction (v_0^x,v_0^y). It can be shown following the procedure provided in [12] that the energy functional (11) is convex in (p,q,v^x,v^y). Hence the following four Euler equations obtained by applying the variational technique to (11) have unique solutions [13]:

$$\left.\begin{aligned} g\nabla^2 p-(1-g)(p+v^x-f_x)=0 \\ g\nabla^2 q-(1-g)(q+v^y-f_y)=0 \end{aligned}\right\} (x,y)\in(D-C)$$

$$\iint_{D-C}(1-g)(p+v^x-f_x)dxdy+\lambda(v^x-v_0^x)=0$$

$$\iint_{D-C}(1-g)(p+v^x-f_x)dxdy+\lambda(v^x-v_0^x)=0$$

$$(p,q)=\mathbf{0}, \text{ when } (x,y)\in\partial C \text{ and } \nabla(p,q)=\mathbf{0}, \text{ when } (x,y)\in\partial D. \quad (12)$$

After solving (12) we revert to the flow-field variables (u,v) through (9) by adding the drift bias to the globally optimal flow (p,q). Finally we use (u,v) as the external force in the snake equation (3) in order to track the fast-rolling leukocytes.

5 TRACKING RESULTS

Adding a shape-size constraint to the snake model helps in tracking the quasi-circular shaped leukocytes *in vivo* [4]. So, for tracking fast leukocytes we use the enhanced GVF flow along with the shape-size constrained snake. For tracking experiments we have chosen those sequences where the leukocytes are moving at speeds greater than 100 μm/s and are considered fast-rolling. To obtain a performance measure of the proposed tracker, we have generated ground truth for the cells first by tracking the sequences manually. Two types of error measure have been considered: *root mean square error* (RMSE) of the tracked cell center positions in microns and *percentage of frames tracked*. If a computed cell center is within one cell radius from the actual cell center, then that frame is tracked. The percentage is computed as the ratio of number of frames tracked to the total number of frames in the sequence. Four types of trackers including the proposed tracker are considered for the purpose of comparison – the centroid tracker [7], the correlation tracker [8], the GVF snake tracker and the enhanced GVF snake tracker.

We have taken 25 fast rolling leukocyte sequences, each 31 frames long (=1 second), from 17 intravital experiments. The RMSE comparison is shown in Figure 7. The proposed snake tracker is seen to have the lowest associated RMSE of all the four trackers. Figure 8 shows that the proposed tracker also yields the highest percentage of frames tracked. The efficacy of the enhanced GVF snake tracker is seen in both the RMSE and percentage tracked measurements.

Acknowledgements: This work has been supported by the Whitaker Foundation.

6 REFERENCES

[1] K. Ley, "Leukocyte recruitment as seen by intravital microscopy," In *Physiology of Inflammation*. K. Ley, editor, New York: Oxford University Press, pp. 303-337, 2001.

[2] N. Manjunath, P. Shankar, B. Stockton, P.D. Dubey, J. Lieberman, U.H. von Andrian, "A transgenic mouse model to analyze CD8+ effector T cell differentiation in vivo," In *Proceedings of the National Academy of Sciences USA*, vol. 96, pp. 13932-13937, 1999.

[3] K.E. Norman, G.P. Anderson, H.C. Kolb, K. Ley, B. Ernst, "Sialyl Lewis^x (sLe^x) and an sLe^x mimetic, CGP69669A, disrupt E-selectin-dependent leukocyte rolling in vivo," *Blood*, vol. 91(2), pp. 475-83, 1998.

[4] N. Ray and S.T. Acton, "Active contours for cell tracking," *Proceedings of IEEE Southwest Symposium on Image Analysis and Interpretation*, IEEE Computer Press, Santa Fe, New Mexico, April 7-9, 2002.

[5] C. Xu and J.L. Prince, "Snakes, shapes, and gradient vector flow," *IEEE Trans. Image Processing* vol. 7, pp. 359-369, 1998.

[6] C. Xu and J.L. Prince, "Generalized gradient vector flow external force for active contours," *Signal Processing*, vol. 71, pp. 131-139, 1998.

[7] R.N. Ghosh and W.W. Webb, "Automated detection and tracking of individual and clustered cell surface low density lipoprotein receptor molecules," *Biophysical Journal*, vol. 66, pp.1301-1318, 1994.

[8] G.J. Schütz, H. Schindler, and Th. Schmidt, "Single-molecule microscopy on model membranes reveals anomalous diffusion," *Biophysical Journal*, vol. 73, pp.1073-1080, 1997.

[9] M. Kass, A. Witkin and D. Terzopoulos, "Snakes: Active contour models," *Proceedings of First International Conference on Computer Vision*, pp. 321-331, 1987.

[10] N. Ray, S. T. Acton, T. Altes and E. E. de Lange, "MRI ventilation analysis by merging parametric active contours," *Proceedings of IEEE ICIP 2001*, pp.861-864, Thessaloniki, Greece, October 2001.

[11] L.D. Cohen and I. Cohen, "Finite-element methods for active contour models and balloons for 2-D and 3-D images," *IEEE Trans. On Pattern analysis and Machine Intelligence*, vol. 15, no. 11, pp. 359-369, 1993.

[12] C. Xu and J. L. Prince, "Global Optimality of Gradient Vector Flow," *Proc. of 34th Annual Conference on Information Sciences and Systems (CISS'00)*, March 2000.

[13] C.A. Hall and T.A. Porsching, *Numerical analysis of partial differential equations*. Englewood Cliffs, New Jersey: Prentice Hall, Inc., 1990.

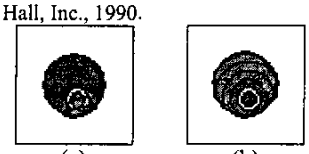

(a) (b)

Figure 1. a) The GVF snake cannot capture the circle boundary (initial snake in white, evolving snakes in black); b) the enhanced GVF snake captures the boundary.

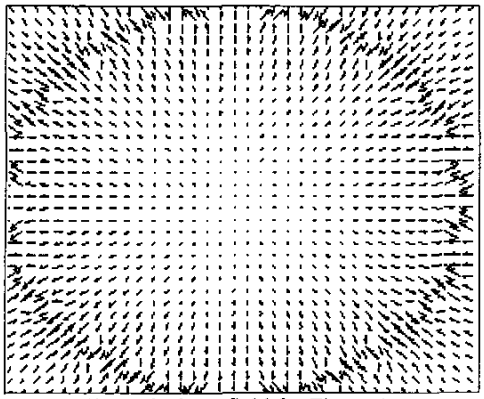

Figure 2. GVF field for Figure 1a.

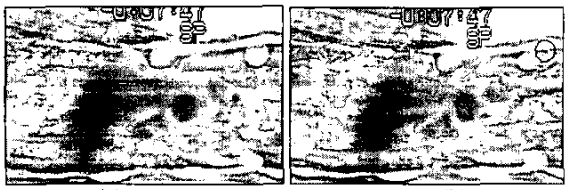

(a) (b)

Figure 3. a) *In vivo* video frame. The tracked cell is delineated by a shape-size constrained [4] snake shown as a white contour; b) GVF snake (equipped with the shape-size constraint) drifts away from the leukocyte.

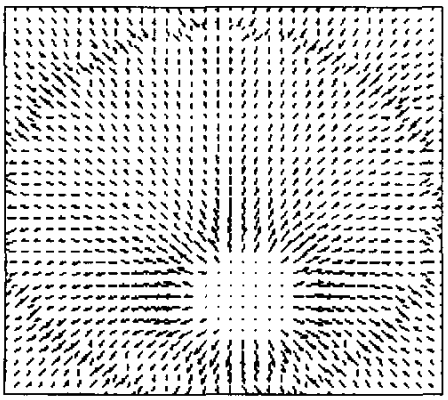

Figure 4. Enhanced GVF field corresponding to Figure 1b.

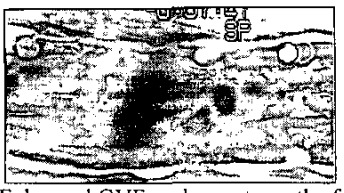

Figure 5. Enhanced GVF snake captures the fast rolling leukocyte. This snake is also constrained by the shape and size criteria [4].

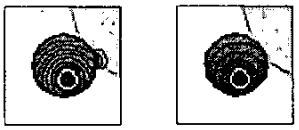

(a) (b)

Figure 6. a) A pressure snake "leaks" through the weak gradient (initial snake in white, evolving snakes in black); b) the enhanced GVF snake can accommodate a combination of strong and weak edges.

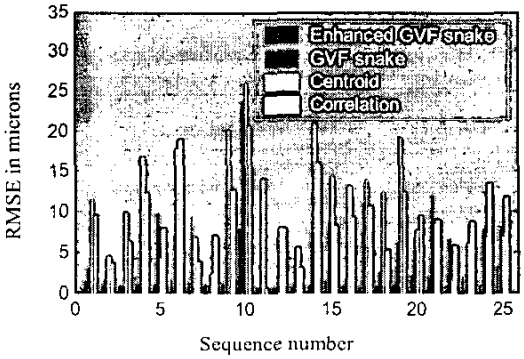

Figure 7. RMSE comparison for the four trackers.

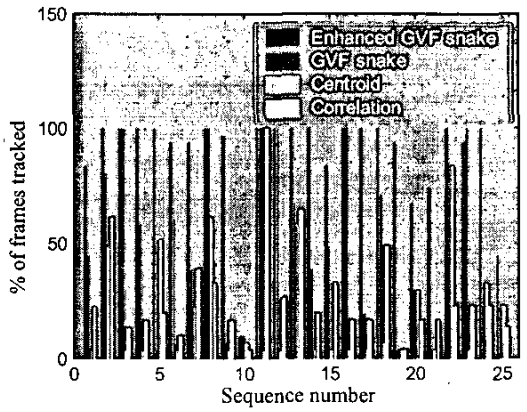

Figure 8. Percentage of frames tracked for the four trackers.